

**Sedimentation Behavior of Coagulated
Suspension of Sodium Montmorillonite
in the Semi-dilute Regime**

July 2016

Mingyu WU

Sedimentation Behavior of Coagulated Suspension of Sodium Montmorillonite in the Semi-dilute Regime

A Dissertation Submitted to
the Graduate School of Life and Environmental Sciences,
the University of Tsukuba
in Partial Fulfillment of the Requirements
for the Degree of Doctoral of Philosophy in Agricultural Science
(Doctoral Program in Appropriate Technology and Sciences for
Sustainable Development)

Mingyu WU

Contents

Chapter 1 Introduction.....	1
1.1 Background.....	1
1.2 Mineralogy and colloidal properties of montmorillonite.....	4
1.3 Sedimentation processes for coagulated clay suspension.....	10
1.4 Thesis objectives.....	13
1.5 Outline of this thesis.....	14
References.....	16

Chapter 3 Effects of electrolyte concentration and pH on the sedimentation rate of coagulated suspension of sodium montmorillonite.....	42
3.1 Introduction.....	42
3.2 Experimental.....	48
3.2.1 Material.....	48
3.2.2 Sample preparation.....	49
3.2.3 Determination of maximum sedimentation rate.....	49
3.2.4 Measurement of ultimate sediment height.....	50
3.3 Results.....	50
3.3.1 Effects of pH and NaCl concentration on maximum velocity of the boundary	50
3.3.2 Effects of pH and NaCl concentration on ultimate sediment height.....	52
3.4 Discussion.....	54
3.4.1 Relation between maximum sedimentation rate and characteristic of equivalent hydrodynamic floc in homo-zone.....	54
3.4.2 Applicability of Michaels-Bolger method.....	58
3.4.3 Extent of deformation of floc influenced by ionic strength	60
3.4.4 Extent of deformation of floc influenced by pH	62
3.5 Conclusion.....	63
References.....	65
Chapter 4 Conclusions and perspectives.....	68
4.1 Conclusions.....	68
4.2 Perspectives.....	70
Publications related to this thesis.....	72
Acknowledgements.....	73

Chapter 3 Effects of electrolyte concentration and pH on the sedimentation rate of coagulated suspension of sodium montmorillonite

3.1 Introduction

Aqueous suspensions of montmorillonite display unique flow characteristics that are useful for technological and agricultural applications such as paints, drilling fluids, ceramics, and soil conditioners [1a, 2]. The macroscopic properties of the montmorillonite suspensions used in these applications are related to the microscopic particle interactions in the suspensions, which are controlled by many factors including chemical ones like pH, and electrolyte type and concentration [3]. Numerous studies have focused on microscopic particle interactions by investigating the rheological behavior of montmorillonite suspensions [4]. There are two classical descriptions of these microscopic structures [5]. One is van Olphen's "card-house" structure that forms through the electrostatic attraction between the negatively charged basal surface and positively charged edges of the structures [1a]. The other is the swelling model proposed by Norrish, who ascribed the formation of microscopic structures to the electric double layer repulsive interaction accompanying hydration forces [6]. However, the applicability of these concepts to the flow characteristics of aqueous montmorillonite suspensions has not yet been adequately verified.

A montmorillonite layer is composed of an octahedral sheet that is sandwiched by two tetrahedral sheets to form a 2:1 structure. Montmorillonite particles are very thin, only 1 nm thick, and have a large basal surface with an average diameter of 500 nm [7]. The basal surfaces carry permanent negative charges with heterogeneous distribution because of random isomorphous substitution (Fig. 3.1). The edges with broken bonds are influenced by pH; i.e., they are able to adsorb protons and hydroxyl ions in keeping with the pH of the medium. Under certain chemical conditions, the

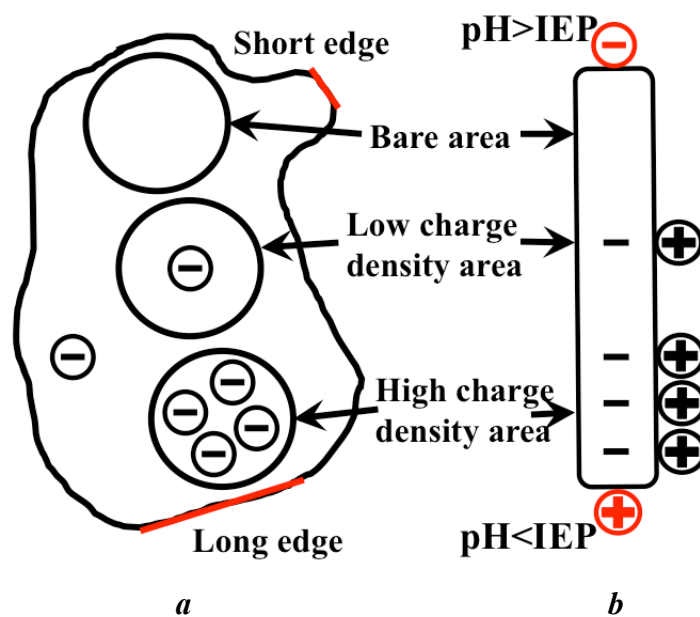


Fig. 3.1 Graphical representation of electronic and morphological properties of montmorillonite particles. (Redrawn from Ref. [25]). *a* Front view of a sodium montmorillonite particle with different length scales for the edge because of the irregular shape and heterogeneous distribution of charge on the basal surface. *b* Side view of a sodium montmorillonite particle with negatively and positively charged edges under alkaline and acidic conditions, respectively. IEP is abbreviation of isoelectric point of edge surface.

expected ideal pure configurations of particle association are edge–face (EF), edge–edge (EE), and face–face (FF). These models have not been observed purely in practical slurries, but can be formed predominantly [1a, 2]. The configuration formed is expected to be primarily ascribed to the particular sedimentation behavior of a flocculated suspension.

The edge of a montmorillonite particle is irregular rather than the theoretical hexagon [8] (Fig. 3.1). The particles can remain individual or form thin packets when the salt concentration is lower than 0.2 M, and the exchangeable cations in the interlayer are replaced with alkali ones [9, 10a]. Compared with kaolin, montmorillonite can easily produce big flocs (Table 3.1). The physical properties of montmorillonite flocs are sensitive to external factors. For operability, it is convenient to control the interaction of montmorillonite particles by modifying their surface chemistry through control of the physicochemical conditions of the medium including pH, and salt type and concentration. Such modification of the surface chemistry of montmorillonite particles changes the force balance between vicinal platelets. The forces between vicinal platelets can be classified as: 1) repulsive forces, like electrostatic repulsive forces caused by contacting surfaces (edge or basal surfaces) with charges of same sign, and short-range hydration forces originating from the hydrated clay surfaces and exchangeable counter cations; and 2) attractive forces, including universal van der Waals forces that induce FF and EE particle association, and electrostatic attractive forces, which result in EF interactions between positively charged edges and negatively charged faces of montmorillonite particles.

These changes on the microscale affect the macroscale behavior of montmorillonite suspensions. Numerous studies have been performed on the rheology of montmorillonite, resulting in two pictures. van Olphen[14] suggested that for concentrated montmorillonite suspensions, at very dilute salt concentrations ($3\text{--}5 \times 10^{-5}$ M NaCl), the effective charge determining the electrostatic attraction between the edge and face lowers. This lowers the Bingham yield stress because the links between the particles decrease, which is termed “internal mutual flocculation”; i.e.,

Table 3.1 Increment ratio of effective volume fraction (α) and diameter of equivalent hydrodynamic floc (d_f) of sodium montmorillonite and kaolin, obtained by Michaels–Bolger (M-B) method [13].

Clay	α	d_f (mm)	Reference
Na-montmorillonite	3363-3991(NaCl 0.5-1.5M, pH10)	0.69-1.80	[11]
Kaolin	65-117(NaCl 0.03-0.5M, pH10)	0.12-0.62	[12]
	35-65(NaCl free-0.06M, pH4-9)	0.099-0.26	[13]

the repulsive potential originating from the electric double layer (EDL) of a face is greater than that of EF interactions. Upon addition of a small amount of NaCl, the Bingham yield stress increases; that is, the EDL of faces is compressed. As a result, the EF attraction is greater than the FF interaction, and the EF association is strengthened. Very high ionic strength causes the Bingham yield stress to decrease again because the FF association of particles dominates, inducing the layered-packing of particles. This decreases the number of links within the matrix, even causing sedimentation (aggregation) in dilute suspensions. Other studies examining the effects of pH and salt concentration on the rheological properties of sodium montmorillonite suspensions support van Olphen's picture [5], [15], [16] and [17].

Callaghan and Ottewill [18] showed the variation of pressure between parallel platelets (FF interaction) over the NaCl range from 10^{-5} to 10^{-1} M arose from the inter-force between particles, and concluded that long-range electrostatic interactions are responsible for the gel properties of montmorillonite dispersions first suggested by Norrish [6]. Later, Rand and Pekenć [19] found no evidence that rheological behavior was affected by pH (4–11) or salt concentration (0–1 M), supporting the existence of EF contact rather than EE and FF associations in montmorillonite dispersions. A study at low salt concentration (< 1 mM) described the spatial and orientational correlations between platelets in an attempt to explain the time-dependent gelation and thixotropic behavior of montmorillonite suspensions [20]. This degree of chaos was semi-theoretically expressed as a function of salt concentration to 10 mM at pH 10, where the EDL developed well [21]. Abend and Lagaly [22] mapped out a sol–gel transient diagram for sodium montmorillonite and defined sol, repulsive gel, attractive gel and floc as fluid states by exposing the sodium montmorillonite to water (unspecified pH; probably ~ 7) at NaCl concentrations ranging from 10^{-5} to 1 M, where the edge was negatively charged. The formation of a repulsive gel is attributed to the electroviscous effect at low ionic strength caused by the well-developed EDL promoting the immobilization of particles. Adding salt induced the E(-)F(-) and E(-)E(-) interactions because of compression of EDL and FF association eventually

dominated flocculation. Tombácz and Szekeres [23] adopted the concept of the spillover effect [24] and summarized the data obtained from X-ray diffraction patterns of montmorillonite films in terms of net proton consumption as a function of pH at different salt concentrations. From the rheological behavior of the films, they concluded that EF heterocoagulation occurs above 25 mM at pH 4, where the screening EDL of positively charged edges emerged. Around the point of zero charge of the edge (pH ~6.5), a higher concentration of salt (~50 mM NaCl) will induce the EF interaction between poorly charged edges and negatively charged faces. Adding 0.1 M or more NaCl at around pH 8 resulted in transient coagulation of FF homo-type interactions.

On the other side of flow behavior of suspensions is sedimentation in the static state. Keren et al. [25] examined the sedimentation behavior of “concentrated” sodium montmorillonite suspensions at pH 5.0, 7.5 and 9.8 near the critical coagulation concentration (CCC), and suggested that EF and EE associations are predominant at pH 5.0 and 7.5, respectively. The high gel volume at pH 9.8 results from an open structure consisting of FF interactions, which forms because the layers are flexible and the permanent charge on faces has a heterogeneous distribution. Miyahara et al. [11] examined the maximum sedimentation rate as a function of volume fraction of solids using the Michaels–Bolger (M-B) method [13] combined with the Richardson–Zaki (R-Z) equation [26] to calculate the equivalent hydrodynamic diameter of floc (d_f) within the sediment and increment ratio of effective volume fraction of the particles (α) caused by the formation of floc at pH 10 with NaCl concentration ranging from 0.5 to 1.5 M. The values of d_f and α increased with salt concentration, and α qualitatively agreed with the values obtained from rheological data [27] evaluated by the Batchelor equation [28]. The increasing trends of d_f and α are ascribed to FF association. With increasing salt concentration, the vicinal platelets approach more closely and form flocs with more irregular shapes.

The effects of both pH and salt concentration on the sedimentation behavior of sodium montmorillonite suspensions are still poorly understood. In this investigation, the range of ionic strength covered extends from near the CCC to very high. The pH

is set to give charged edges with a high charge density. In this case, the physicochemical conditions that affect the surface chemistry and sedimentation behavior of sodium montmorillonite suspensions are expected to change the microstructure of particle association resulting from the different force balance. The present study also attempts to find some evidence for the existence of EF contact between neighboring particles. According to different CCC values from previous studies [10b] at diverse conditions of pH and solid contents, 50 mM NaCl was considered as the onset of salt concentration of the suspension in present study. The protonation and deprotonation reactions only take place on the edge surface, where the pH-dependent sites are located. When the pH 6.5 is regarded as the IEP for the edge surfaces [23], the pH of suspension was set at 4 ± 0.3 and 9.5 ± 0.3 was considered that the edges were highly charged positively and negatively, respectively. At these pHs, the probability of EE contact is very low as well as the edge-face heterocoagulation (EF interaction) and face-face homocoagulation (FF interaction) are expected respectively.

3.2 Experimental

3.2.1 Materials

High-purity Kunipia-F montmorillonite powder was obtained from Kunimine Co. Ltd., Tokyo. The detailed sodium-saturation method for the stock suspension followed the procedure adopted in previous studies [7], [11] and [27]. As describing in section 2.2.2, the preparing steps for the saturating procedures respectively proceeded: dispersing the powder into distilled water, sedimentation for 5.3 days, exchanging the layer cations in high NaCl solution, dialyzing the extra NaCl, and storing at 4 °C in refrigerator.

3.2.2 Sample preparation

With the similarity of section 2.2.3, the all samples in this chapter were made as: The initial height of the suspension was 15.8 cm and diameter of cylinder was 5.0 cm, which were consistence with the previous study [11]. pH 4 ± 0.3 and 9.5 ± 0.3 denote the edge charged positively and negatively, respectively [23]. NaCl was varied from 50mM initially denotes closing to the critical coagulation concentration (CCC) [10b]. The mixtures are rotated end-over-end at 5 times with a frequency 2 s/rotation, followed 1 min ultrasonication with intensity of 100kHz, which of time was included in settling process. The suspension was immersed into water with a part of 85 mm from the bottom of cylinder. The location of the clear boundary was visually recorded at the elapsed time. The relation between these boundary location and elapsed time plotted the sedimentation curves at each chemical condition (pH and ionic strength).

3.2.3 Determination of maximum sedimentation rate

As classified in section 1.3 [29], under certain external conditions of primary particles, with increasing solid concentration, a visible boundary between slurry and supernatant is formed and maintains its shape throughout the whole sedimentation process. This can be regarded as a zone settling sedimentation pattern, and begins at semi-dilute particle concentration. The maximum velocity of the boundary in the acceleration period almost reflects the elimination rate of the homogeneous zone.

We assumed that the dispersed particles form a rigid, spherical floc in the physicochemical environment. The value of α can be calculated from the volume fraction of floc to that of primary particles (Eq. 3.1) by postulating that the homogeneous zone consists of these flocs under compression-free conditions compared with the consolidation zone, where the sediment experiences the self-weight of the sediment. Then, the sedimentation of the homogeneous zone can be

regarded as hindered settling. The maximum sediment rate, which is calculated as the maximum slope of the relatively linear portion of the settling curve, obeys the R-Z method (Eq. 3.2). Using the M-B method, α is obtained from the slope of the maximum velocity as a function of solid concentration (Eq. 3.3).

$$\alpha = \frac{\phi_f}{\phi_p} \quad (3.1)$$

$$Q = V_S(1 - \phi_f)^{4.65} \quad (3.2)$$

$$Q^{1/4.65} = V_S^{1/4.65}(1 - \alpha\phi_p) \quad (3.3)$$

where ϕ_f and ϕ_p denote the volume fraction of floc and primary particles, respectively, Q is the velocity of the boundary, and V_S is the terminal velocity of floc.

3.2.4 Measurement of ultimate sediment height

Because the diameter of the cylinder does not influence the sediment height, measurement of ultimate sediment height was performed under the same chemical conditions using the same pretreatment procedure with volume fractions of solids of 1.155×10^{-4} and 2.31×10^{-4} under a gravitational field. The initial height of the slurry was 200 mm. Normally, after a sedimentation time of 31 days, the height of a sediment is considered constant [27].

3.3 Results

3.3.1 Effects of pH and NaCl concentration on maximum velocity of the boundary

The maximum velocity of the boundary (Q) for the homogeneous zone as a function of salt concentration at pH 4 and 9.5, and the relative difference in percentage (RDP) of Q as a function of pH at different NaCl concentration are presented in Fig. 3.2. At different pH and the same ionic strength, the RDP values

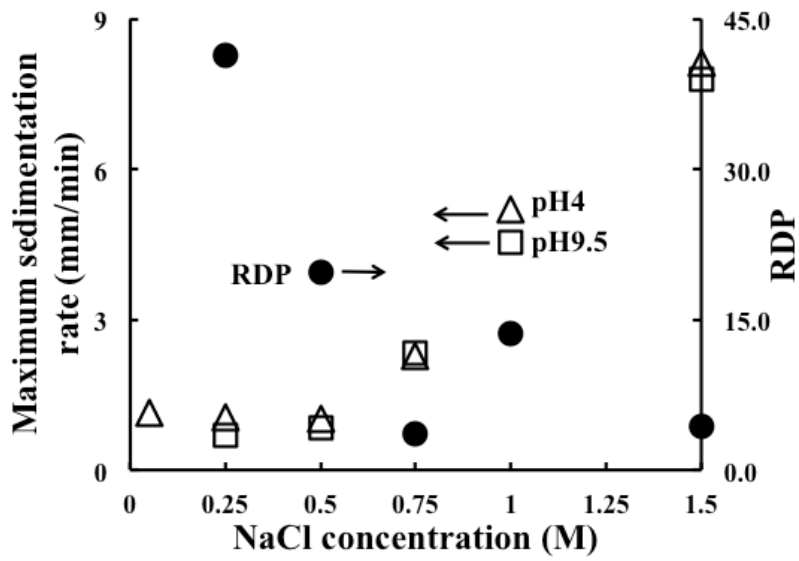


Fig. 3.2 Maximum velocity of boundary (Q , mm/min) for the zone settling stage as a function of NaCl concentration at different pH (referencing to left vertical axis). Relative difference in percentage (RDP) of Q as a function of pH at different NaCl concentration (referencing to right vertical axis). $H_0=15.8$ cm, $D_0=5.0$ cm, volume fraction of primary particles: $\phi=1.097 \times 10^{-4}$.

were calculated as the percentage of the absolute value of the difference between one of the maximum velocities and their average value to the average value [30]. The results demonstrate that the maximum velocities increase with NaCl concentration. Although the difference of the velocities as a function of pH at fixed NaCl concentration is small, the RDP values depended strongly on NaCl concentration, but were below 5% at 0.75 M NaCl. That is, the influence of pH on Q is greater at low NaCl concentrations but is almost negligible at high ones.

3.3.2. Effects of pH and NaCl concentration on ultimate sediment height

The ultimate sediment height of suspensions at different pH as a function of salt concentration is plotted in Fig. 3.3. Except the height at pH 9.5 and 50 mM NaCl, the other plots show similar tendencies because chemical factors strongly influence the sediment height; that is, the trends induced by the chemical factors followed two different models when we set 0.25–0.5 M NaCl as an inflection range. For NaCl concentrations less than 0.25 M, with increasing NaCl concentration, the sediment height decreases under acidic conditions and increases under alkaline conditions at $\phi_1=1.155 \times 10^{-4}$, and the former is of greater magnitude than the latter. In contrast, when the NaCl concentration exceeded 0.5 M, the sediment height increased with NaCl concentration. The sediment heights were slightly higher for alkaline samples than acidic ones. Additionally, the turning point of the properties of sodium montmorillonite particles at 0.3 M NaCl observed by Norrish is located in the present inflection range. The trend observed under acidic conditions as a function of ionic strength is similar to that found by van Olphen [1b], even though the samples were probably treated under neutral conditions, and the sedimentation time was 2 months.

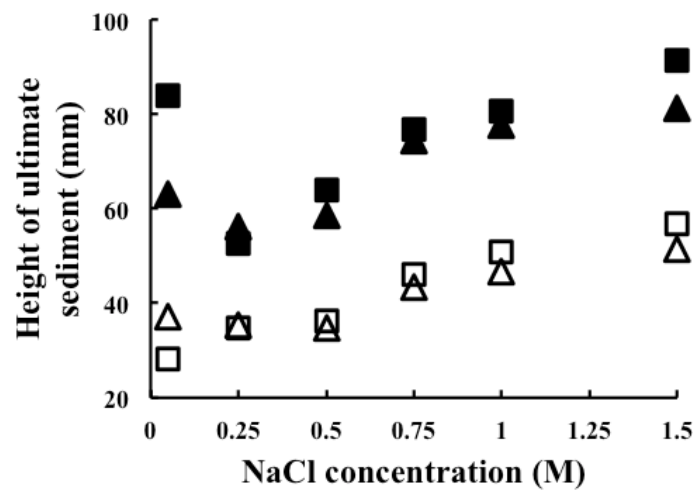


Fig. 3.3 The height of ultimate sediment (sedimentation time: 31 days) as function of NaCl concentration at different pH. $H_0=200$ mm, $D_0=50$ mm, $\phi_1=1.155 \times 10^{-4}$, $\phi_2=2.31 \times 10^{-4}$. \triangle pH4 ϕ_1 , \square pH9.5 ϕ_1 ; \blacktriangle pH4 ϕ_2 , \blacksquare pH9.5 ϕ_2 .

3.4 Discussion

3.4.1 Relation between maximum sedimentation rate and characteristic of equivalent hydrodynamic floc in homo-zone

Normally, the sedimentation behavior of dispersions reflects some characteristics of the components within the aqueous media; for instance, bigger and denser particulates can accelerate the settling velocity, and a low volume fraction of particles can decrease the interference degree in hindered settling. It was assumed that samples in this study were all in the laminar flow regime, and obeyed the Stokes formula. Based on Eq. 3.2, we plotted $Q^{1/4.65}$ against ϕ_p (Fig. 3.4) to obtain α and d_f values as a function of NaCl concentration at different pH, as illustrated in Figs. 3.5 and 3.6, respectively. The α values ranged from 1748 to 4905 in this study and thus are greater than that of kaolin by at least one order of magnitude, as summarized in Table 3.1. The d_f values are located in the range of 0.52–1.04 mm and are also larger than those of kaolin. These observations can be attributed to the unique shape parameters of montmorillonite particles, such as higher aspect ratio, and thinner edge thickness than the corresponding values of kaolin. Because α is inversely related to floc density, the trends exhibited in Figs. 3.5 and 3.6 can be used to determine the size and density of flocs induced under different pH and salt concentration conditions. When the NaCl concentration exceeds 0.5 M, the size and density of flocs qualitatively agree with those at maximum sedimentation rate, as shown in Fig. 3.2. That is, as salt concentration increases, the size and density of flocs also increases, which leads to a higher maximum sedimentation rate. From Figs. 3.5 and 3.6, these two parameters in this ionic strength region are not affected by pH. However, different behavior is observed in the region of low salt concentration (below 0.5 M NaCl), where the slight decrease and increase of the maximum sedimentation rate with increasing in salt concentration takes places at pH 4 and 9.5 respectively. In the meanwhile, the downtrend of d_f with salt concentration (Fig. 3.6) was similarly observed by Chang

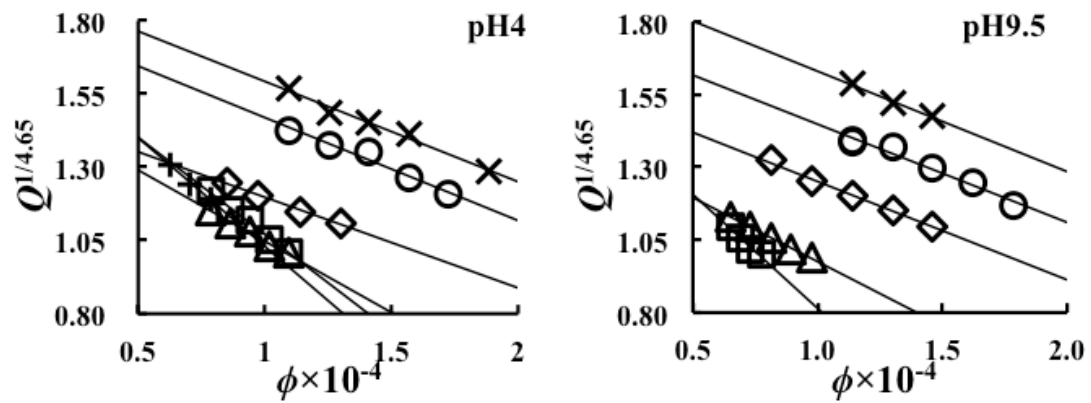


Fig. 3.4 Plots of $Q^{1/4.65}$ against ϕ_p used to calculate α as a function of NaCl concentration under acidic (pH 4) and alkaline (pH 9.5) conditions. The NaCl concentrations are denoted as: +:0.05M, \square :0.25M, \triangle :0.5M, \diamond :0.75M, \circ :1.0M, \times :1.5M. $H_0=158$ mm, $D_0=50$ mm.

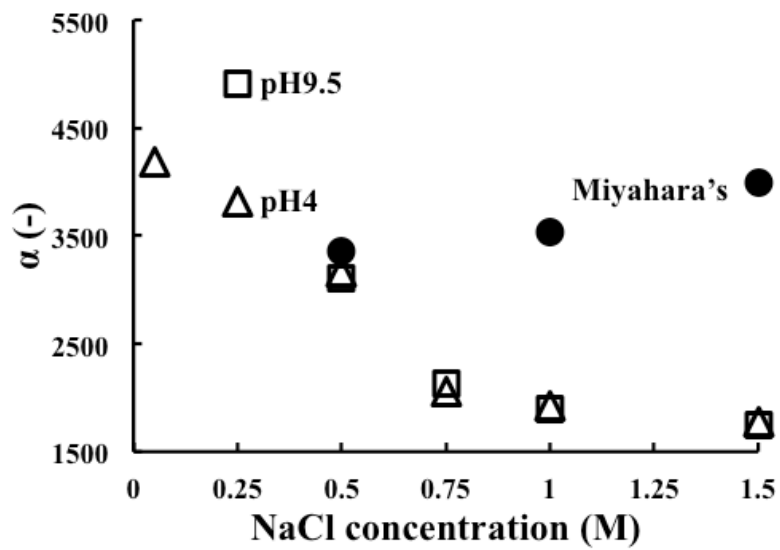


Fig. 3.5 Variation of the increment ratio of effective volume fraction (α) in homogeneous zone using the M-B method as a function of NaCl concentration at different pH. $H_0=158$ mm, $D_0=50$ mm. The symbol, Miyahara's "•", denotes the data after Ref. [11] with similar size of cylinder, pH10 and the NaCl varied at 0.5, 1.0, 1.5M.

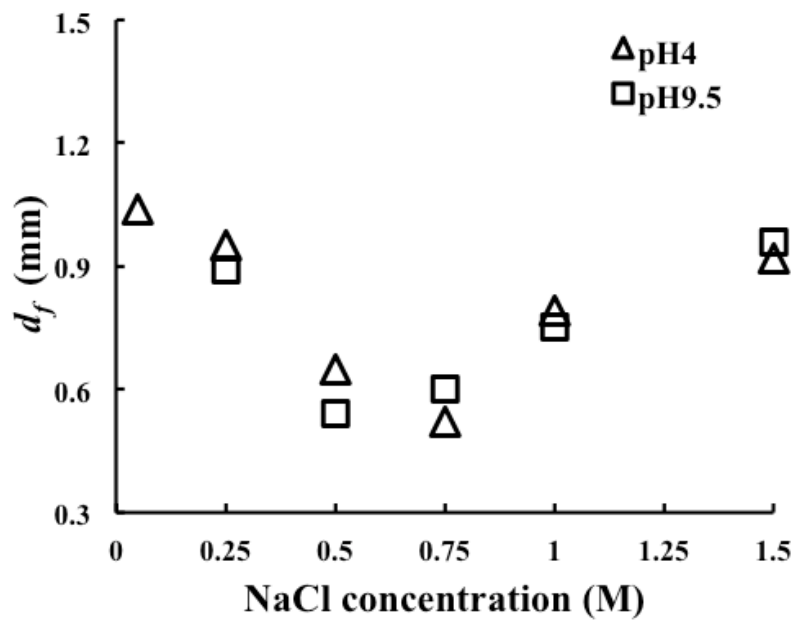


Fig. 3.6 Variation of the diameter of equivalent hydrodynamic floc (d_f) in homogeneous zone using the Stokes' formula as a function of NaCl concentration at different pH. $H_0=158$ mm, $D_0=50$ mm.

and Leong [31], but the variations of d_f and α with ionic strength at both pHs cannot be consistent with that of maximum sedimentation rate in this range of salt concentration. Therefore, the validity of M-B method on semi-dilute sodium montmorillonite suspension in the low salt concentration region is doubtful and the applicability of M-B method beyond the two ionic strength regimes should be further investigated.

3.4.2 Applicability of Michaels-Bolger method

Viewing Fig. 3.6 again reveals that the d_f values of 0.89 mm (pH 9.5) and 0.95 mm (pH 4) at an ionic strength of 0.25 M are similar to those of 0.96 mm (pH 9.5) and 0.92 mm (pH 4) at 1.5 M NaCl. Unfortunately, in the zone settling stage, the sediment morphology strongly depended on ionic strength, as indicated in Fig. 3.7. In Fig. 3.7, the sediment observed at lower salt concentration is more homogeneous compared with those at higher salt concentration. That is, at lower ionic strength, the equivalent flocs within the sediment in the zone settling stage are obviously smaller than those at higher ionic strength. Additionally, Fig. 3.5 indicates that at pH 9.5, α decreases from 3111 (0.5 M) to 1748 (1.5 M). The opposite trend, *i.e.*, an increase of α with salt concentration, was observed by Miyahara [11] under similar conditions (pH 10, diameter of cylinder 5.0 cm, initial height of suspension 15.8 cm). However, the ultrasonication intensity was different from that used on our samples. These factors are primitive, however, the strict control is not easy.

In the range of ionic strength higher than 0.5 M NaCl, an upward trend of floc diameter was demonstrated. This trend confirms the result of our previous research [11], however, it opposes to the data reported Chang and Leong's [31], *i.e.*, the mean particle size decreases from a maximum at 0.1 M NaCl to a minimum at 0.5 M NaCl. This difference can be ascribed to the difference in volume fraction of particles. The volume fraction of our system ($\sim \times 10^{-4}$) is less by two orders of magnitude than that of Chang and Leong ($\sim \times 10^{-2}$). In such high volume fraction, the growth of aggregate

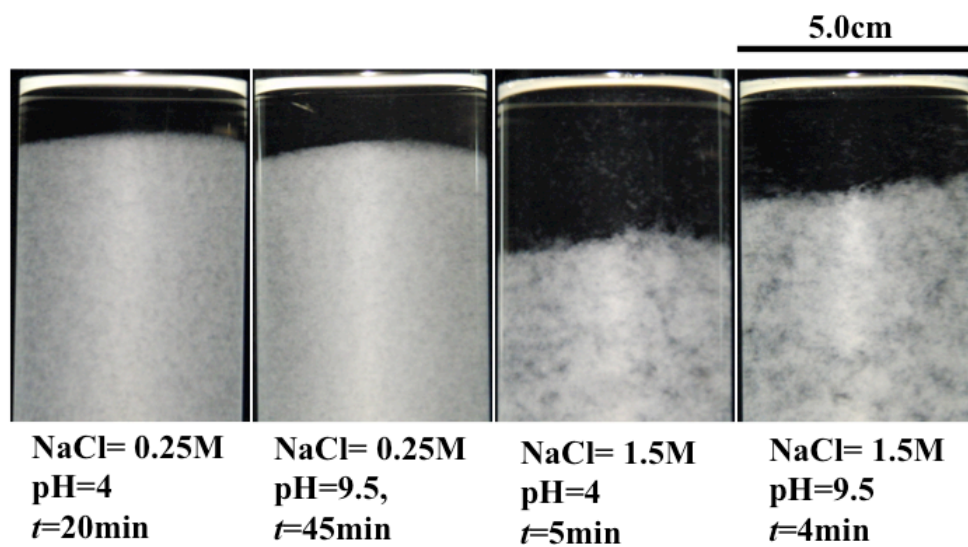


Fig. 3.7 Photos of upper part of suspension taken under various chemical conditions when the boundary experienced maximum settling velocity. $H_0=158$ mm, $D_0=50$ mm, and $\phi=1.097 \times 10^{-4}$. t denotes the time from starting the measurement to the photo taken. The “white top” in each sample scales as 5.0 cm and denotes the boundary between the supernatant and air.

will be interfered by the presence of neighbors resulting more compact structure than the system of dilute suspension. If we define this factor as a structure factor in the sediment mass, the size of floc in the sediment can be regarded to be determined reflecting the factor of cohesive force and the factor of structure. Even within the region of the dilute suspension, the presence of such two factors can be referred [32]. We think that the condition of maximum size reported by Chang and Leong (0.1 M NaCl) corresponds to the optimum condition of the product of the two factors, while our result obtained much lower concentration is reflected just by cohesive forces. Further investigation to reveal the quantitative explanation should be done in future.

3.4.3 Extent of deformation of floc influenced by ionic strength

The ultimate sediment is formed after almost finishing the consolidation process in the gravitational field; the height of this sediment is determined by self-weight. Under conditions of pH 9.5 and NaCl 50 mM, the suspension is near the CCC [10b]. In this case, the Debye length of a particle is approximately 1.36 nm, which is comparable with the edge thickness of 1 nm; that is, the influence of the EDL on the effective volume of the particles cannot be neglected. The suspension turns into an “attractive gel” [22], in which the degree of particle orientation and localization is limited by the primary volume fraction of solids because of the high aspect ratio and very thin edge of particles. That is, at low solid concentrations, because of the higher degree of freedom in the settling process, the particles are able to arrange more parallel, so the ultimate sediment height is lower than that at higher solid concentration, as shown for a solid concentration of $\phi_1 = 1.155 \times 10^{-4}$ in Fig. 3.3. Conversely, the lower degree of freedom for the particles at “high” solid concentration of $\phi_2 = 2.31 \times 10^{-4}$ arising from the resistance between neighboring particles produces a higher ultimate sediment height.

With rising salt concentration, the EDL changes from shielding to completely removal, allowing the vicinal platelets to approach each other more closely. In this

sense, the increase of ultimate sediment height should reflect the strength of the network composed of the weakly contacting particles. If we assume that the network consisted of equivalent hydrodynamic flocs, the ultimate sediment height reflects the extent of deformation of the flocs for the transition from the homogeneous zone to the consolidation zone under the condition that the suspension possesses the same amount of solids. In the present study, the samples prepared under alkaline conditions possess negatively charged edges, the extent of which decreases as salt concentration increases, consistent with Miyahara's findings [27]. That is, at low ionic strength, which is defined as less than the inflection range in this study, the long-range electrostatic repulsion is larger than the universal attraction, causing the vicinal particles to separate. This separation gives rise to a large α and loose floc. Conversely, the degree of freedom of particles is also large enough to allow particles to rotate and localize easily, so the deposit forms a more parallel array than that at high ionic strength. The ultimate sediment height is low, and the deformation of the floc between the homogeneous zone (denoted as α in Fig. 6, $\phi_1 = 1.155 \times 10^{-4}$) and consolidation zone (denoted as ultimate sediment height in Fig. 3.3) is large when the solid content in the suspension is low. This repulsion weakened as ionic strength increased, so the particles approach each other more closely. As a result, the degree of freedom of particles decreased and the flocs strengthened. Therefore, less deformation leads to increased ultimate sediment height. At very high NaCl concentration, such as over 0.5 M in this study, the approach of neighboring particles should be explained in another way; *i.e.*, according to the Norrish transition point (0.3 M NaCl) of the swelling of sodium montmorillonite layers, the repulsive forces controlling the separation between platelets are predominantly long-range electrostatic repulsion and short-range hydration repulsion originating from exchangeable cations. Further increasing the ionic strength caused the amount of bulk solvent around the cations to decrease [33], and the hydration number of water molecules around the cations also diminished [34] and [35]. This allows the platelets to get closer, so the structure becomes more stable. The ultimate sediment height increased with NaCl concentration.

3.4.4 Extent of deformation of floc influenced by pH

The trend of ultimate sediment height under acidic conditions is different from that under alkaline conditions. Particle association is more complicated to form the “card-house” structure when the pH of suspension is below the isoelectric point of edge surface than when the pH is above. In this study, the edges were considered positively charged at pH 4. Also, a NaCl concentration of 50 mM exceeded the CCC[10b]; *i.e.*, an EDL originating from positively charged edges emerged. In such a case, EF association is probable. Under acidic conditions (pH 4), the dependence of ultimate sediment height on salt concentration was similar to that observed by van Olphen, even though the pH value in their study was ~ 7 . Because the sedimentation time was 2 months in van Olphen’s study, the edges may be weakly positively charged because of adsorption of the released silica and alumina from the particles [36].

Fig. 3.3 shows that a transition of ultimate sediment height occurs in the salt concentration range of 0.25–0.5 M at pH 4. At low salt concentrations, the height decreased with increasing ionic strength. This phenomenon can probably be explained as follows. The irregular shape of particles combined with the heterogeneous distribution of charge density on the particle face can strengthen the E(+)F(–) bonds. Under critical conditions, the weak EF bond involves short edges and low-charge-density areas; the strong EF one includes long edges and high-charge-density areas. As discussed above, under alkaline conditions, with increasing salt concentration at low ionic strength, the EDL of particles diminished, allowing the particles to approach more closely and strengthening the structure. In the ultimate sediment, the particle association endures the particle self-weight as well as the additional resultant force arising from the approaching faces, which disrupts the weak EF bonds within “card-house” structure of particle association. Therefore, the sediment height lowered with addition of salt. Also, at the same ionic strength, the height under acidic conditions is higher than that under alkaline conditions. This may

be attributed to the more stable EF bonds in “card-house” structure under acidic condition than FF configuration at alkaline condition restricting the mobility of the particles and increasing their resistance to deformation caused by their self-weight. Alternatively, at high salt concentration (≥ 0.5 M NaCl), the increase of sediment height with ionic strength under acidic conditions is similar to that found under alkaline ones, which may be explained by the reasoning described above. However, the stepwise increase of the difference of the height with pH at the same ionic strength probably indicates the existence of strong EF bonds even at very high salt concentration. Additionally, because of the doubt regarding the applicability of the M-B method at low salt concentration, a reasonable explanation for the remarkable RDP values in this range should be determined.

3.5 Conclusion

The work presented here shows the effects of pH and ionic strength on sedimentation behavior, including maximum sedimentation rate and ultimate sediment height, for semi-dilute suspensions of sodium montmorillonite. NaCl concentration extending to near the CCC (50 mM) and pH of 4 and 9.5 were investigated. The volume fraction of solids was lowered to minus four orders of magnitude, and α caused by the formation of equivalent hydrodynamic flocs was estimated using the M-B method with the R-Z equation using maximum sedimentation rate in zone settling stage. The influences of pH and salt concentration on ultimate sediment height and α were used to examine the relation between the macroscopic sedimentation behavior and microscopic structure of particle association. The results indicated that the effect of pH on the ultimate sediment height was considerable at low ionic strength and almost negligible at high ionic strength with 0.25–0.5 M NaCl as an inflection range. Increasing salt concentration accelerated the maximum sedimentation rate. This can be explained by increasing salt concentration decreasing the repulsive electrostatic effect, breaking of weak EF bonds and residual strong EF bonds. However, the applicability of the M-B method to semi-dilute

suspensions of sodium montmorillonite should be further confirmed. This issue should be studied in the future.

References

- [1] van Olphen, An introduction to clay colloid chemistry, second ed., John Wiley & Sons Inc. London, 1977. a:pp. 95-108; b: pp.121-125.
- [2] G. Lagaly, S. Ziesmer, Colloid chemistry of clay minerals: the coagulation of montmorillonite dispersions, *Adv. Colloid Interface Sci.* 100-102 (2003) 105-128.
- [3] S. Swartzen-Allen, E. Matijevic, Surface and colloid chemistry of clays, *Chem. Rev.* 74 (1974) 385-400.
- [4] P. F. Luckham, S. Rossi, The colloidal and rheological properties of bentonite suspensions, *Adv. Colloid Interface Sci.* 82 (1999) 43-92.
- [5] D. Heath, Th. F. Tadros, Influence of pH, electrolyte, and poly (vinyl alcohol) addition on the rheological characteristics of aqueous dispersions of sodium montmorillonite, *J. Colloid Interface Sci.* 93 (1983) 307-319.
- [6] K. Norrish, The swelling of montmorillonite, *Discuss. Faraday Soc.* 18 (1954) 120-134.
- [7] Y. Adachi, K. Nakaishi, M. Tamaki, Viscosity of a dilute suspension of sodium montmorillonite in a electrostatically stable condition, *J. Colloid Interface Sci.* 198(1998)100-105.
- [8] J. Zou, A. C. Pierre, Scanning electron microscopy observations of “card-house” structures in montmorillonite gels, *J. Mater. Sci. Lett.* 11 (1992) 664-665.
- [9] H. Vali, L. Bachmann, Ultrastructure and flow behavior of colloidal smectite dispersions, *J. Colloid Interface Sci.* 126(1988) 278-291.
- [10] F. Bergaya, G.Lagaly, *Handbook of Clay Science, Part A: Fundamentals*, Second ed., Elsevier Ltd. Amsterdam, 2013. a: pp. 243-328; b: pp.266-274.
- [11] K. Miyahara, M. Ohtsubo, K. Nakaishi, Y. Adachi, Sedimentation rate of sodium montmorillonite suspension under high ionic strength, *Nendo Kagaku (Journal of the Clay Science Society of Japan)*, 40 (2001) 179-184. (in Japanese with English abstract)
- [12] Y. Kuroda, K. Nakaishi, R. Shibata, The influence of salt concentration on

structure of kaolinite floc, *Nendo Kagaku (Journal of the Clay Science Society of Japan)*, 37(1998) 137-143. (in Japanese with English abstract)

[13] A. S. Michaels, J. C. Bolger, Settling rates and sediment volumes of flocculated kaolin suspensions, *Ind. Eng. Chem. Fundam.* 1(1962) 24-33.

[14] H. van Olphen, Internal mutual flocculation in clay suspensions, *J. Colloid Sci.* 19 (1964) 313-322.

[15] R. K. Khandal, Th. F. Tadros, Application of viscoelastic measurements to the investigation of the swelling of sodium montmorillonite suspensions, *J. Colloid Interface Sci.* 125 (1988) 122-128.

[16] R. Sohm, Th.F Tadros, Viscoelastic properties of sodium montmorillonite (Gelwhite H) suspensions, *J. Colloid Interface Sci.* 132 (1989) 62-71.

[17] F. Miano, M.R. Rabaioli, Rheological scaling of montmorillonite suspensions: the effect of electrolytes and polyelectrolytes, *Colloids Surf. A.* 84 (1994) 229–237.

[18] I. C. Callaghan, R. H. Ottewill, Interparticle forces in montmorillonite gels, *Faraday Discuss. Chem. Soc.* 57 (1974) 110-118.

[19] B. Rand, E. Pekenć, J. W. Goodwin, R. W. Smith, Investigation into the existence of edge—face coagulated structures in Na-montmorillonite suspensions, *J. Chem. Soc., Faraday Trans. 1*, 76 (1980) 225-235.

[20] J. D. F. Ramsay, P. Lindner, Small-angle neutron scattering investigations of the structure of thixotropic dispersions of smectite clay colloids, *J. Chem. Soc., Faraday Trans.* 89 (1993) 4207-4214.

[21] N. Sakairi, M. Kobayashi, Y. Adachi, Effects of salt concentration on the yield stress of sodium montmorillonite suspension, *J. Colloid Interface Sci.* 283 (2005) 245–250.

[22] S. Abend, G. Lagaly, Sol–gel transitions of sodium montmorillonite dispersions, *Appl. Clay Sci.* 16 (2000) 201–227.

[23] E. Tombácz, M. Szekeres, Colloidal behavior of aqueous montmorillonite suspensions: the specific role of pH in the presence of indifferent electrolytes, *Appl. Clay Sci.* 27 (2004) 75–94.

[24] R. B. Secor, C. J. Radke, Spillover of the diffuse double layer on

- montmorillonite particles, *J. Colloid Interface Sci.* 103 (1985) 237-244.
- [25] R. Keren, I. Shainberg, Eva Klein, Settling and flocculation value of sodium-montmorillonite particles in aqueous media, *Soil Sci. Soc. Am. J.* 52 (1988) 76-80.
- [26] J. F. Richardson, W. N. Zaki, Sedimentation and fluidization: part 1. *Trans. Inst. Chem. Eng.* 32 (1954) 35-53.
- [27] K. Miyahara, Y. Adachi, K. Nakaishi, The viscosity of a dilute suspension of sodium montmorillonite in an alkaline state, *Colloids Surf., A*, 131(1998) 69-75.
- [28] G. K. Batchelor, The effect of Brownian motion on the bulk stress in a suspension of spherical particles, *J. Fluid Mech.* 83 (1977) 97-117.
- [29] G. Imai, Settling behavior of clay suspension, *Soils and Foundations*, 20 (1980) 61-77.
- [30] Shujian Xiang, A discussion to some methods of calculation for relative difference, *Journal of Zhongnan University of Economics*, 4 (1996) 91-94. (in Chinese)
- [31] W. Z. Chang, Y. K. Leong, Ageing and collapse of bentonite gels—effects of Li, Na, K and Cs ions, *Rheol. Acta.* 53 (2014) 109–122.
- [32] M. Kobayashi, Y. Adachi, and S. Ooi, Breakup of fractal flocs in a turbulent flow, *Langmuir*, 15 (1999) 4351–4356.
- [33] Y. Marcus, On water structure in concentrated salt solutions, *J. Solution Chem.* 38 (2009) 513-516.
- [34] Y. Marcus, Concentration dependence of ionic hydration numbers, *J. Phys. Chem. B*, 118 (2014) 10471–10476.
- [35] D.W. McCall, D. C. Douglass, The effect of ions on the self-diffusion of water. I. Concentration dependence, *J. Phys. Chem.* 69 (1965) 2001–2011.
- [36] P. Bar-On, I. Shainberg, Hydrolysis and decomposition of na-montmorillonite in distilled water, *Soil Sci.* 109 (1970) 241-246.